CONF-790306--3

LA-UR-78-2932

TITLE: IRRADIATION PERFORMANCE OF HELIUM-BONDED URANIUM-PLUTONIUM CARBIDE FUEL ELEMENTS

MASTER

AUTHOR(S): T. W. Latimer (LASL)
R. L. Petty (LASL)
J. F. Kerrisk (LASL)
N. S. DeMuth (LASL)
P. J. Levine (W-ARD)
A. Boltax (W-ARD)

SUBMITTED TO:

Monterey International Conference on
Fast Breeder Reactor Fuel Performance
March 5-8, 1979

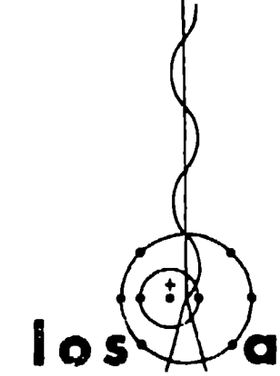

los alamos
scientific laboratory
of the University of California
LOS ALAMOS, NEW MEXICO 87545

An Affirmative Action/Equal Opportunity Employer

Form No. 836
St. No. 2629
1/75

UNITED STATES
ENERGY RESEARCH AND
DEVELOPMENT ADMINISTRATION
CONTRACT W-7405-ENG. 36

IRRADIATION PERFORMANCE OF HELIUM-BONDED URANIUM-PLUTONIUM CARBIDE FUEL ELEMENTS

T. W. Latimer, R. L. Petty, J. F. Kerrisk, and N. S. DeMuth (LASL)
P. J. Levine and A. Boltax (W-ARD)

INTRODUCTION

The current U.S. program on advanced carbide and nitride fuels is part of the Advanced LMFBR Fuels Development Program initiated in 1974. A summary of the U.S. experience related to the irradiation testing of carbide fuels in EBR-II during 1965-1974 was presented at the International Meeting on Advanced LMFBR Fuels in October 1977.[1] One major phase of the current program is the steady-state irradiation testing of various designs of helium-bonded uranium-plutonium carbide fuel elements. A total of 171 helium-bonded carbide elements (plus replacements for interim examinations) are included in this testing phase. These elements were fabricated by the Los Alamos Scientific Laboratory (LASL) and the Westinghouse Advanced Reactors Division (W-ARD).

DESCRIPTION OF IRRADIATION TESTS

The helium-bonded carbide elements are either 7.87- or 9.40-mm in diameter and employ combinations of 81 or 87% T.D. fuel with 0.13-0.15 mm or 0.25-0.28 mm fuel-cladding diametral gaps. The fuel is predominantly $(U_{0.8}Pu_{0.2})C + 10 \pm 5\% (U,Pu)_2C_3$. The majority of the elements are clad in 0.51-mm-thick, 20% cold-worked Type 316 stainless steel; 59 elements are clad in 0.38-mm- or 0.51-mm-thick solution-treated Nimonic PE16. The designs for these elements resulted from the evaluation of 76 helium-bonded carbide fuel elements irradiated in EBR-II as part of early screening tests during 1965-1974.[1,2] The experimental design and operating parameters of the current tests are shown in Table I. The irradiation conditions for these tests simulate those anticipated in the top end of a Fast Test Reactor (FTR) fuel element where maximum cladding temperatures occur (Series K8, K9, and K10) as well as in the middle of an FTR element where peak power is generated.

TABLE I

Design and Operating Parameters for Helium-Bonded Carbide Fuel Elements

Series[a]	No. of Elements	Design Parameters: Fuel Density (% T.D.)	Diam. Gap (mm)	Smear Density (% T.D.)	Cladding Type[e]	Operating Parameters: Peak Power (kW/m)	Peak Cladding Temp. (°C)	Goal Burnup (at.%)	Status[h] Peak Burnup (at.%)
				7.87-mm Diameter, 0.51-mm Cladding Thickness					
K6A	9	81	0.13	78	316-I	75	565	12	7.9-11.3
	10	81	0.25	75	316-I				
K6B	16[b]	87	0.25	81	316-I	75	565	12	5.9-12.4
	3	81	0.13	78	316-I				
K7	5	87	0.25	81	316-N	75	595	12	8.1-9.1
	4	81	0.13	78	316-N				
	4	81	0.25	75	316-N				
WSA-31	7	87	0.13	84	PE16	75	595	12	4.5-4.8
	6	87	0.25	81	PE16				
	6	87	0.25	81	316-N				
WSA-34	4	87	0.13	84	PE16[f]	75	595	12	1.0-1.2
	4	87[c]	0.13	81	PE16				
	4	87[d]	0.13	75	PE16				
	7	87	0.25	81	PE16				
K8	5	87	0.25	81	316-N	45	650	8	4.0-4.2
	4	81	0.13	78	316-N				
	4	81	0.25	75	316-N				
				9.40-mm Diameter, 0.51-mm Cladding Thickness					
WSA-32	4	87	0.28	81	316-N	100	595	12	7.7-8.7
	5	87	0.28	81	316-IV				
	5	81	0.15	78	316-IV				
	5	81	0.28	76	316-IV				
WSA-33	8	87	0.15	84	PE16[g]	100	595	12	2.3-3.2
	8	87	0.28	81	PE16[g]				
	3	87	0.28	81	316-IV				
K9	4	87	0.28	81	316-IV	70	655	8	3.5-3.7
	4	81	0.15	78	316-IV				
	4	81	0.28	76	316-IV				
K10	5	87	0.15	84	PE16	70	655	8	4.0-4.9
	5	87	0.28	81	PE16				
	5	87	0.28	81	316-N				
	4	87	0.28	81	316-IV				

[a] K Series are LASL-sponsored; WSA Series are W-ARD sponsored.

[b] Six elements contain 0-2 vol% M_2C_3.

[c] 1.27-mm-i.d. annular pellet.

[d] 2.16-mm-i.d. annular pellet.

[e] 316 = 20% cold-worked Type 316 stainless steel;
N = N-lot; I = first core; IV = fourth core;
PE16 = solution-treated Nimonic PE16 formed by drawing.

[f] Rolled before solution-annealing for 4 elements.

[g] 4 elements have 0.38-mm cladding thickness.

[h] At end of ESR-II run 35 (August 1978).

STATUS OF IRRADIATION TESTS

As of August 1, 1978, 15 of the original 171 helium-bonded carbide elements had reached their goal burnups. In addition, 25 elements were removed, at burnups of 4-9 at.%, for interim destructive examinations and for transient overpower tests. A total of 66 elements had attained burnups of 8-12 at.%. A cladding breach has been identified in one element. The peak burnup attained by each series is shown in Table I.

RESULTS OF POSTIRRADIATION EXAMINATIONS

Only four elements from Series K6A and K6B have completed postirradiation examinations. These postirradiation results and a description of the elements are given in Table II.

Fuel Restructuring

Three or four metallographic sections each from elements K6A-52, K6A-61, K6B-74, and K6B-91 were examined. No unusual features were noted in any of the metallographic sections or in the autoradiographs. Midplane sections of the three elements containing hyperstoichiometric fuel--K6B-91 (88% T.D. fuel, 0.25-mm diametral gap), K6A-52 (81% T.D. fuel, 0.13 mm diametral gap), and K6A-61 (82% T.D. fuel, 0.25-mm diametral gap)--are shown in Fig. 1.

TABLE II

Postirradiation Results from K6A and K6B Fuel Elements

Element No.	K6A-52	K6A-61	K6B-74	K6B-91
Fuel Type	MC+9%M_2C_3	MC+8%M_2C_3	MC+1%M_2C_3	MC+9%M_2C_3
Fuel Density (% T.D.)	81	82	88	88
Diam Gap (mm)	0.13	0.25	0.25	0.25
BOL Peak Power (kW/m)	64	66	68	71
Peak Burnup (at.%)	7.87	8.41	5.93	6.15
Fission-Gas Release (%)	12.5	19.0	8.5	7.9
Max Clad ΔD/D (%)	0.90	0.46	0.71	0.65
Max Clad Swelling (% ΔD/D)	0.13	0.11	0.02	0.03
Max Mech. Strain (%)	0.77	0.35	0.69	0.62

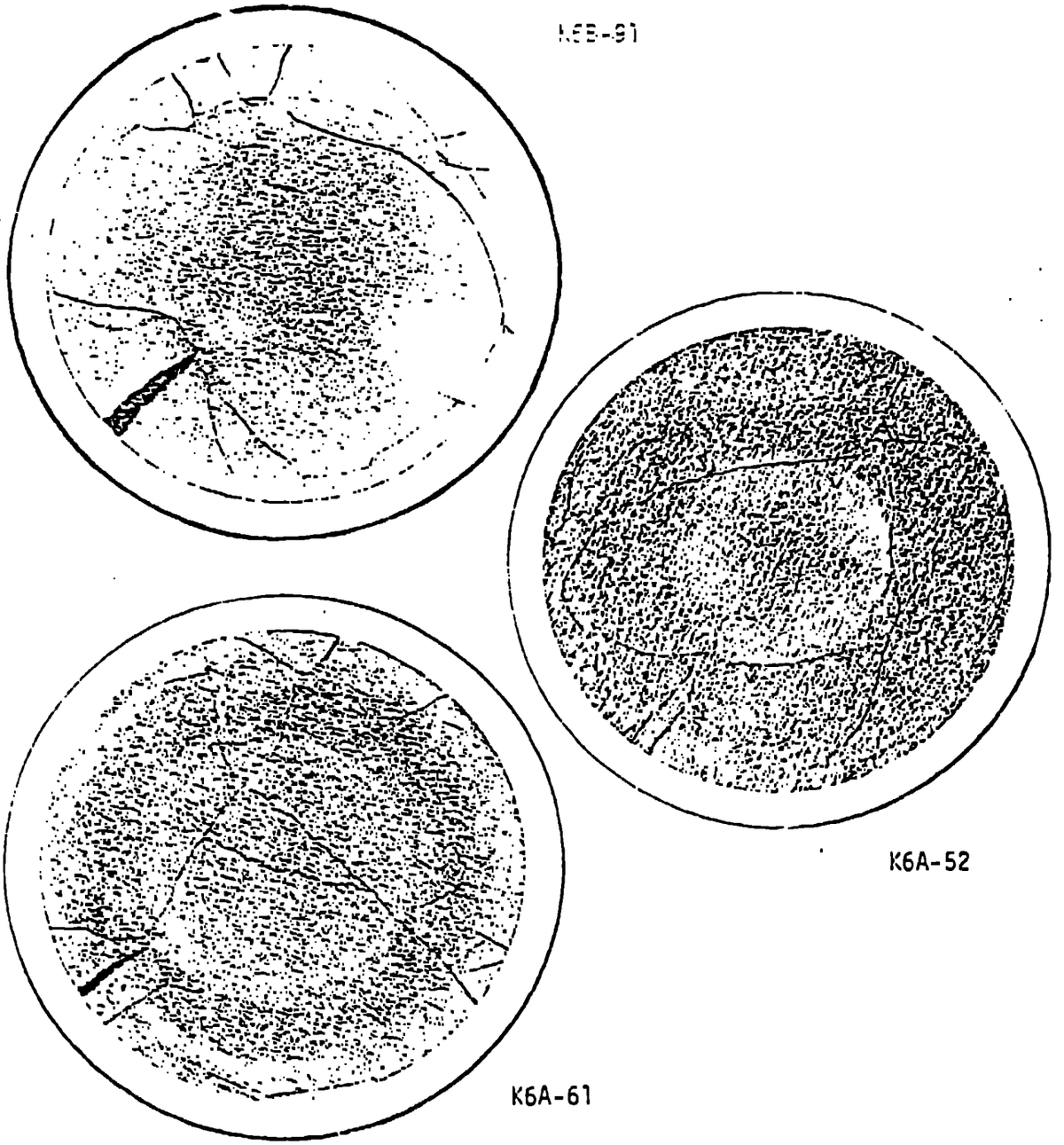

Fig. 1. Midplane transverse sections of elements K6B-91, K6A-52, and K6A-61. (As polished.)

Little difference was observed in the metallography and autoradiography of elements K6B-74 (stoichiometric fuel) and K6B-91 (hyperstoichiometric fuel). The average diameters of the porous inner zones of the sections taken near the top, middle, and bottom of the fuel stacks were 63-67% of the cladding inside diameter. The high-intensity β-γ rings, showing the increased concentrations of fission products, were within the areas of the porous zones and correlated well with the locations of the boundaries of the porous zones. The β-γ rings were less distinct in the bottom sections. The central portions of the fuel in all sections were depleted of fission products. The large radial fuel cracks were closed in the central porous zone as a result of fuel swelling; they remained only in the outer unrestructured zone. The smaller fuel cracks appeared to be the result of thermal stresses being relieved during cooldown. The longitudinal sections showed that, in the central porous zone, the fuel pellets were sintered together. Compared to K6B-91, the cross-section of K6A-52 indicated a greater tendency to use the available space provided by the original fuel-cladding gap. The lack of any large radial cracks near the inside cladding surface and the highly symmetric shape of the porous inner zone are particularly noteworthy. Although the smear density was 3% less than that of K6B-91, the average diameter of the central porous zone in K6A-52 was only 46% of the cladding inside diameter, significantly less than that of K6B-91. The cross section of K6A-61 also demonstrated the increased ability of the lower density fuel to swell into available space provided by the original fuel-cladding gap. However, the lower smear density and higher fuel operating temperatures of K6A-61, compared to K6A-52, caused more extensive and complex fuel restructuring. The average diameter of the restructured zone of the midplane section of K6A-61 was 82% of the cladding inside diameter. In addition, two porous zones were observed, each of which showed regions of fuel densification at the outer boundaries. The β-γ autoradiographs showed a significantly larger and less symmetric central zone depleted of fission products in K6A-61 than in K6A-52. A thin ring of increased α activity that was coincident with the high-intensity β-γ ring in both K6A-52 and K6A-61 was observed. This may be the result of fuel densification in a thin layer at the edge of the inner porous zone.

Fission-Gas Release

As previously observed in helium-bonded carbide elements[1,2] fission-gas release was inversely related to smear density. The fission-gas releases for Series K6A and K6B elements of 81, 78, and 75% smear density were 8%, 13%, and 19%, respectively. However, the fission gas releases for these types of elements were only about half of the releases found for elements with similar smear densities and operating conditions in earlier EBR-II screening tests.[1,2] These differences may be due to differences in oxygen contents, which were typically less than 500 ppm in the Series K6A and K6B fuels compared to 1100-4400 ppm in the earlier experiments.

Cladding Strain

The maximum cladding strains measured at the interim examinations of the Series K6A, K6B, K7, and WSA-31 elements are shown in Fig. 2. In all comparisons of elements of the same series and clad in the same alloy, maximum cladding strains were directly related to the smear densities of the elements. In the only experiment to determine the effect of fuel stoichiometry, the elements containing stoichiometric (U,Pu)C showed a somewhat higher average cladding strain than comparable elements containing ~10 vol% $(U,Pu)_2C_3$. Although the elements of comparable design clad in N-lot 20%-cold-worked Type 316 stainless steel appear in Fig. 2 to have higher cladding strains than elements clad in Core-I steel, the elements clad in N-lot steel operated at a 30°C higher cladding temperature so a direct comparison of cladding behavior is not yet available.

Cladding-density measurements were available for elements from the K6A and K6B Series. Cladding swelling was quite low; 0.05-0.08 vol% for the K6B elements at a fluence of 3.8-3.9 x 10^{22} n/cm^2 (E > 0.1 MeV) and a

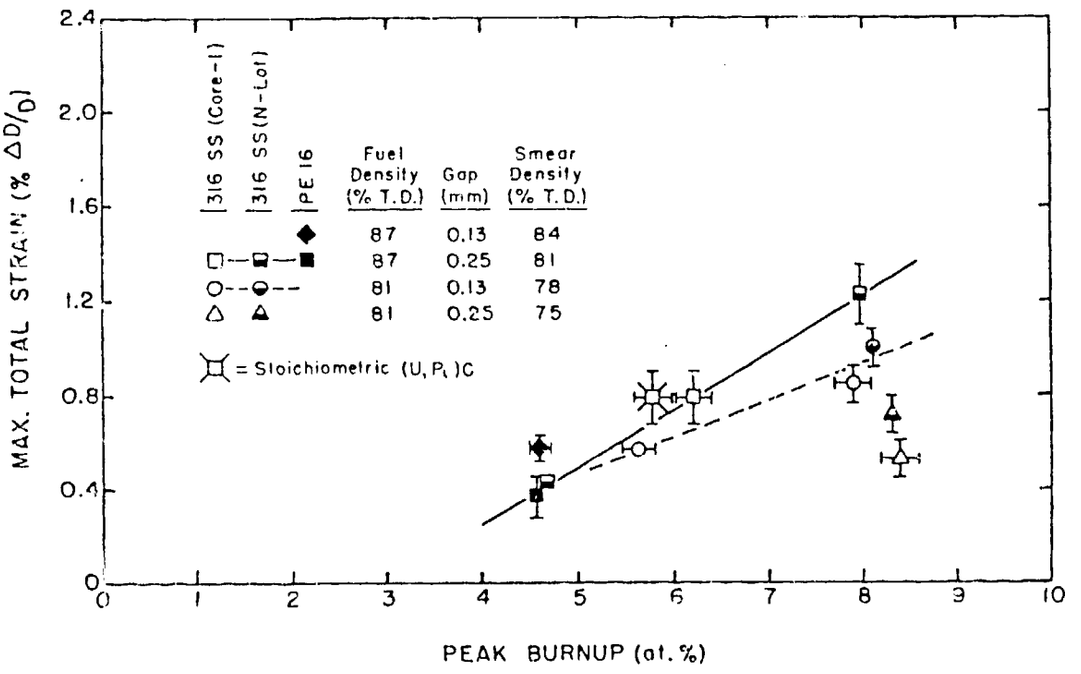

Fig. 2. Maximum cladding strain vs peak burnup for K6A, K6B, K7, and WSA-31 Series helium-bonded carbide fuel elements.

peak temperature of 560-575°C, and 0.33-0.38 vol% for the K6A elements at a fluence of 5.1-5.5 x 10^{22} n/cm^2 and a peak temperature of 565-570°C.

Fuel-Cladding Mechanical Interaction

Figure 2 illustrates the maximum average cladding strains, which are due almost entirely to fuel-cladding mechanical interaction, as a function of peak burnup. Although average cladding strain is generally used as the primary measure of fuel-cladding mechanical interaction, it is evident from other measurements that forces in addition to cladding stresses caused by fuel swelling could be significant. Additional stresses are inherent in the experiment designs; the K7 and WSA-31 elements were wire-wrapped while the K6A and K6B elements were not wire-wrapped but rather were irradiated in individual flow tubes.

One measure of fuel-cladding interaction is the size and/or frequency of cladding ovalities as measured by two profilometry traces taken 90° apart. These ovalities possibly reflect changes in fuel pellets as they fracture, rearrange, and resinter during reactor startups and steady-state operation. Plots that correlate pellet-interface positions with profilometry traces taken 90° apart show that the ovalities tend to occur over a whole number of pellets (but random in number). Past experience, however, has shown little correlation between the size of the maximum ovalities and reactor operating parameters or failure locations.[2]

Profilometry traces obtained by averaging four diameters (45° apart) at 0.25-mm intervals have revealed differences in fuel-cladding mechanical interaction for the various combinations of fuel density and gap size. Profilometry traces for K6A-52 and K6B-91 are shown in Figs. 3 and 4. The axial position in these figures is the distance from the bottom of the element. The vertical ticks at the top and bottom of each plot represent the pellet-interface positions. The ovalities are not reflected in these average-diameter plots. In both plots, the pellet-interface positions correlate with minima in the profilometry curves. In Fig. 3, the diametral increases associated with each pellet in element K6A-52 (81% T.D. fuel, 0.13-mm diametral gap) tend to be more regular in shape, and there are marked diametral increases at the top and bottom of the fuel stack. In Fig. 4, the diametral increases associated with each pellet in element K6B-91 (88% T.D. fuel, 0.25-mm diametral gap) tend to show double maxima (pellet "hour-glassing"), and the increases at the top and bottom of the fuel stack are less pronounced.

Measurements of individual pellet-interface positions from betatron radiographs were made for two Series K6A elements and four Series K6B elements. These measurements were compared with pre-irradiation values. The element that showed the largest increase in fuel-stack length (2.81 mm)

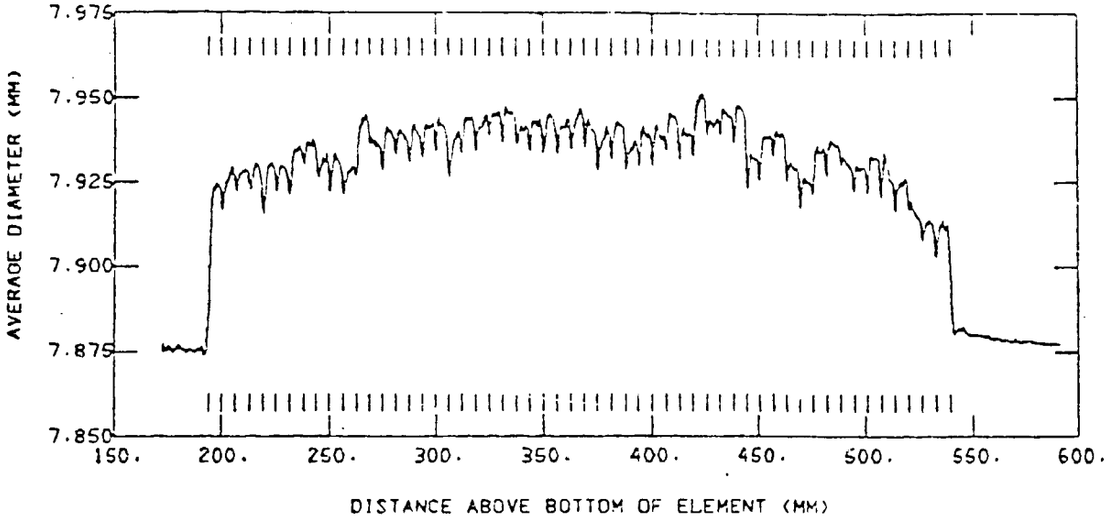

Fig. 3. Profilometry and fuel-pellet-interface positions for element K6A-52

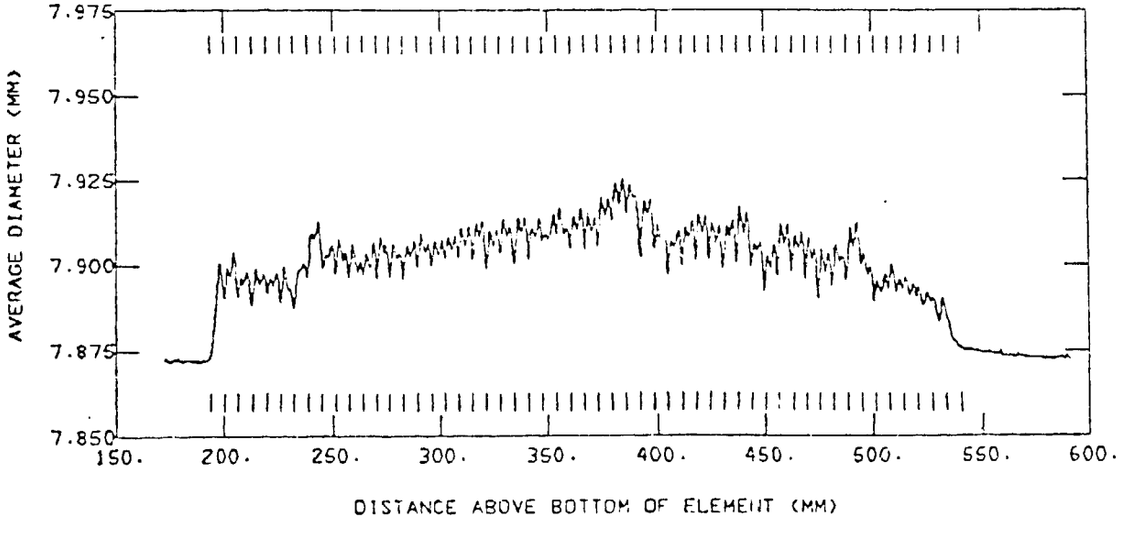

Fig. 4. Profilometry and fuel-pellet-interface positions for element K6B-91.

was K6A-52 (81% T.D. fuel), which had the smallest original diametral gap and the lowest beginning-of-life (BOL) fuel temperature (~1500°C). Element K6A-61, which had a 0.25-mm diametral gap and a correspondingly higher BOL temperature (~1900°C) showed only a slight increase of 0.20 mm in the fuel-stack length with a negative difference throughout most of the fuel-stack length. This is further evidence of some fuel densification in element K6A-61.

Of the elements containing 87% T.D. fuel with 0.25-mm diametral gaps, the three incorporating two-phase fuel showed some negative differences in the lower part of the fuel stack but overall increases of 0.99, 2.18, and 2.46 mm. A greater amount of fuel densification occurred in the element containing single-phase fuel which showed shrinkage throughout the fuel-stack length and an overall decrease of 0.33 mm. The BOL central fuel temperatures of these four elements were 1800-1850°C.

In the K7 Series, the helium-bonded elements containing 87% T.D. fuel with 0.25-mm diametral gaps showed pronounced bulging at the ends of the fuel pellets (sometimes as many as 10-15 pellets) at the top of the fuel stacks. In contrast, in elements containing 81% T.D. fuel with a 0.25-mm diametral gap, less pronounced bulging was observed and only in the top 3-5 pellets. No pellet bulging was observed in elements containing 81% T.D. fuel with a 0.13-mm diametral gap.

It is evident that many interaction mechanisms are taking place between carbide fuel pellets and the cladding. Evidence is shown by size and frequency of ovalities, pellet "hour-glassing", size of increase at the ends of the fuel stack, axial length changes, and degree of axial restraint of the fuel pellets. Examination of the elements of the current irradiation program at their goal burnups are expected to clarify the relative importance of these interaction processes.

Fuel-Cladding Chemical Interaction

Although essentially no fuel-cladding gap remained after ~6 at.% burnup in K6B-74 and K6B-91, there were only a few areas where interaction zones were observed. These areas were found in the midplane and bottom sections of both elements. The interaction zones were similar in appearance to zones observed previously in other helium-bonded carbide elements,[2] and in out-of-pile compatibility tests,[3,4] and identified as containing primarily nickel and plutonium as well as some iron and uranium. The maximum depths of these interaction zones in K6B-74 and K6B-91 were 8 μm.

After ~8 at.% burnup, with no fuel-cladding gap remaining in K6A-52, the maximum depth of the interaction zones in any section was 2 μm. A 13-17 μm gap over ~120° of the fuel-cladding interface in K6A-61 showed

increased α activity and contained a plutonium-enriched phase containing fission products, but no attack of the cladding was observed in the areas where it was present.

Metallography and microhardness measurements taken at the midplanes of K6B-91 and K6A-52 showed evidence of slight carburization and hardening of the cladding within 40 μm of the fuel-cladding interface. Slight carburization and hardening of 20% cold-worked Type 316 stainless steel has been observed in out-of-pile compatibility tests after contact with (U,Pu)C + 9 vol% $(U,Pu)_2C_3$ for 1000 h at 725°C. No hardening was found near the fuel-cladding interface in K6B-74, which contained only 1 vol% $(U,Pu)_2C_3$.

As observed in previously examined helium-bonded elements, increased α activity was found on the inside surface of the cladding near the ends of large fuel cracks. This has been found to be the result of the presence of americium, as well as plutonium. However, no chemical attack of the cladding was observed in these areas.

Cladding Breach

The WSA-31 test was identified as containing a suspect breached fuel element during run 92B in EBR-II. The assembly was subsequently discharged and disassembled in the Hot Fuel Examination Facility, where a cladding breach was observed in peripheral element W31-17. This element contained 87% T.D. fuel with a 0.13-mm diametral gap and was clad in Nimonic PE16; it attained a peak burnup of 4.8 at.%. The 15-mm-long breach was located directly beneath the spacer wire, 18 mm below the fuel-column midplane where the wire contacted an adjacent fuel element. Evaluation of the fuel-element behavior using the LIFE-3C computer code indicated a low probability that the fuel element breached solely as a result of fuel-cladding mechanical interaction. Two other potential causes of the breach are being investigated: excessive element-bundle interaction force and the metallurgical character of the Nimonic PE16 cladding, which exhibited low ductility and contained longitudinal stringers of carbide precipitates with associated voids. Destructive examination of the pin is currently in progress.

SUMMARY

The current irradiation program of helium-bonded uranium-plutonium carbide elements is achieving its original goals. By August 1978, 15 of the original 171 helium-bonded elements had reached their goal burnups including one that had reached the highest burnup of any uranium-plutonium

carbide element in the U.S.--12.4 at.%. A total of 66 elements had attained burnups over 8 at.%. Only one cladding breach had been identified at that time.

In addition, the systematic and coordinated approach to the current steady-state irradiation tests is yielding much needed information on the behavior of helium-bonded carbide fuel elements that was not available from the screening tests (1965-1974). The use of hyperstoichiometric (U,Pu)C containing ~10 vol% $(U,Pu)_2C_3$ appears to combine lower swelling with only a slightly greater tendency to carburize the cladding than single phase (U,Pu)C. The selected designs are providing data on the relationship between the experimental parameters of fuel density, fuel-cladding gap size, and cladding type and various fuel-cladding mechanical interaction mechanisms.

REFERENCES

1. J. O. Barner, T. W. Latimer, J. F. Kerrisk, R. L. Petty, and J. L. Green, "Advanced Carbide Fuels--U.S. Experience," Advanced LMFBR Fuels, ERDA 4455, pp. 268-298 (1977).

2. T. W. Latimer, J. O. Barner, J. F. Kerrisk, and J. L. Green, "Post-irradiation Results and Evaluation of Helium-Bonded Uranium-Plutonium Carbide Fuel Elements Irradiated in EBR-II--Interim Report," LA-6249-MS (April 1976).

3. T. W. Latimer, "Compatibility of Uranium-Plutonium Carbide Fuels and Potential LMFBR Cladding Materials," ANL-7827 (September 1971).

4. T. W. Latimer and J. F. Andrew, "Compatibility of Helium- and Sodium-Bonded Hyperstoichiometric (U,Pu)C with Advanced Cladding Alloys," Advanced LMFBR Fuels, ERDA 4455, pp. 205-217 (1977).

5. A. Boltax, U. P. Nayak, R. J. Skalka, and A. Biancheria, "Performance Analysis of Helium-Bonded Carbide and Nitride Fuel Pins," International Conference on Fast Breeder Reactor Fuel Performance, Monterey, California, March 5-8, 1979.